JACC: BASIC TO TRANSLATIONAL SCIENCE VOL. 7, NO. 11, 2022

ORIGINAL RESEARCH - PRECLINICAL

Novel GSK-3β Inhibitor Neopetroside A Protects Against Murine Myocardial Ischemia/Reperfusion Injury

Hyoung Kyu Kim, PhD,[a,b,*] Min Kim, PhD,[a,c,*] Jubert C. Marquez, PhD,[a,b,*] Seung Hun Jeong, PhD,[a,c,*] Tae Hee Ko, PhD,[a,c] Yeon Hee Noh, MS,[a,c] Pham Trong Kha, PhD,[a,c] Ha Min Choi, BS,[a,c] Dong Hyun Kim, PhD,[d] Jong Tae Kim, PhD,[e] Young Il Yang, PhD,[e] Kyung Soo Ko, PhD,[a,b] Byoung Doo Rhee, PhD,[a,b] Larisa K. Shubina, PhD,[f] Tatyana N. Makarieva, PhD,[f] Dmitry Y. Yashunsky, PhD,[g] Alexey G. Gerbst, PhD,[g] Nikolay E. Nifantiev, PhD,[g] Valentin A. Stonik, PhD,[f] Jin Han, PhD[a,b,c]

VISUAL ABSTRACT

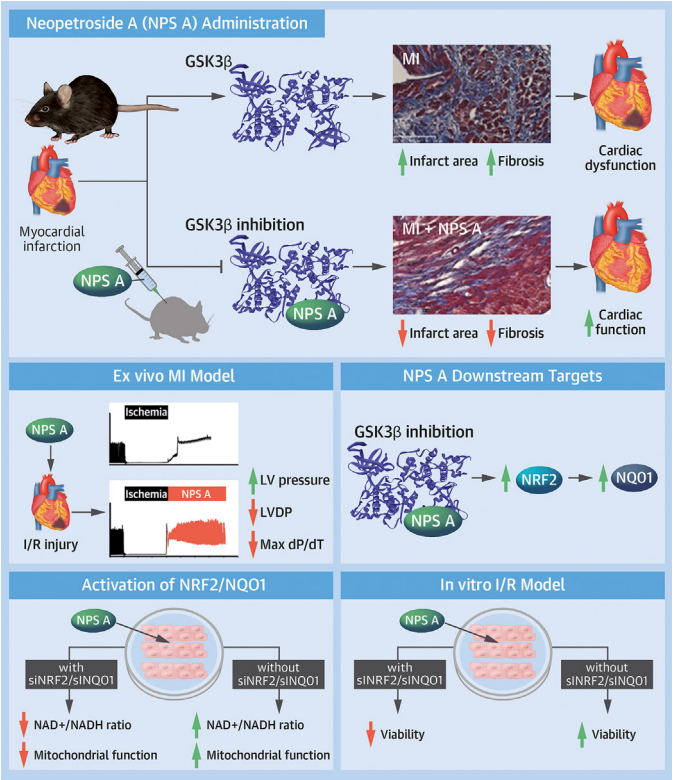

Kim HK, et al. J Am Coll Cardiol Basic Trans Science. 2022;7(11):1102–1116.

HIGHLIGHTS

- **Neopetroside A preserved cardiac hemodynamics and mitochondrial respiration capacity ex vivo after ischemia/reperfusion injury in rat hearts.**
- **NPS A significantly prevented cardiac fibrosis in vivo in myocardial infarcted mice.**
- **In vivo and ex vivo effects were caused by preserved mitochondrial function.**
- **In vitro kinase screening assays, in silico docking simulation studies, and SPR binding assays demonstrated that NPS A directly interacts with GSK-3β.**
- **GSK-3β inhibition regulates the NAD^+/NADH ratio by activating the Nrf2/Nqo1 axis in a phosphorylation-independent manner.**

From the [a]Cardiovascular and Metabolic Disease Center, Inje University, Busan, South Korea; [b]Department of Health Sciences and Technology, Graduate School, Inje University, Busan, South Korea; [c]Department of Physiology, BK Plus Project Team, College of Medicine, Inje University, Busan, South Korea; [d]Department of Pharmacology and Pharmaco-Genomics Research Center, College of Medicine, Inje University, Busan, South Korea; [e]Paik Institute for Clinical Research, Inje University College of Medicine, Busan,

ISSN 2452-302X https://doi.org/10.1016/j.jacbts.2022.05.004

SUMMARY

Recent trends suggest novel natural compounds as promising treatments for cardiovascular disease. The authors examined how neopetroside A, a natural pyridine nucleoside containing an α-glycoside bond, regulates mitochondrial metabolism and heart function and investigated its cardioprotective role against ischemia/reperfusion injury. Neopetroside A treatment maintained cardiac hemodynamic status and mitochondrial respiration capacity and significantly prevented cardiac fibrosis in murine models. These effects can be attributed to preserved cellular and mitochondrial function caused by the inhibition of glycogen synthase kinase-3 beta, which regulates the ratio of nicotinamide adenine dinucleotide to nicotinamide adenine dinucleotide, reduced, through activation of the nuclear factor erythroid 2–related factor 2/NAD(P)H quinone oxidoreductase 1 axis in a phosphorylation-independent manner. (J Am Coll Cardiol Basic Trans Science 2022;7:1102–1116)

ABBREVIATIONS AND ACRONYMS

ATP = adenosine triphosphate

GSK-3 = glycogen synthase kinase-3

I/R = ischemia/reperfusion

MI = myocardial infarction

mPTP = mitochondrial permeability transition pore

mTOR = mammalian target of rapamycin

NAD^+ = nicotinamide adenine dinucleotide

NADH = nicotinamide adenine dinucleotide, reduced

NPS A = neopetroside A

Nqo1 = NAD(P)H:quinone oxidoreductase 1

Nrf2 = nuclear factor erythroid 2-related factor 2

OCR = oxygen consumption rate

Ischemia/reperfusion (I/R) injury causes structural and functional changes in cardiomyocytes, disrupting their mitochondrial function and inducing myocardial damage. Mitochondria are essential regulators of cellular biogenesis, and environmental stimuli such as oxygen tension, hormones, and nutrients are critical for their function and homeostasis.[1] Thus, protecting mitochondrial function to enhance cardiac energy supply is considered to be the primary function of next-generation therapeutics for heart failure.[2] Investigation of novel natural products and their effects on mitochondrial function during or after I/R injury may lead to new pharmaceutical approaches for cardiovascular disease treatment.

Sponges belonging to the genus *Neopetrosia* contain diverse bioactive metabolites.[3] In a previous study, we isolated 2 new pyridine nucleosides from *Neopetrosia* sp, both containing α-glycosidic bonds and an acyl substituent at C-5′. One of these nucleosides, neopetroside A (NPS A), differed from its isomeric analog (β-NPS A) only at the β-glycoside bond.[4] In the same study, we showed that NPS A improved mitochondrial function without cytotoxicity. Considering the ability of NPS A to regulate mitochondria, we hypothesized that this compound would be promising for the treatment of cardiovascular disease.

Cellular metabolism involves several mitochondrial processes, many of which require the universal cofactor nicotinamide adenine dinucleotide (NAD^+). NAD^+ is a coenzyme composed of 2 nucleotides joined by their respective phosphate groups: an adenine base and a nicotinamide.[5] Oxidation of mitochondrial NAD^+, reduced (NADH), occurs when its electrons are donated to complex I (NADH:ubiquinone oxidoreductase) of the electron transport chain.[6] F_0F_1-adenosine triphosphate (ATP) synthesis allows the re-entry of protons into the matrix and is important for driving ATP synthesis. NADH and NAD^+ are vital to the formation of ATP and must be held in an optimal ratio to maintain mitochondrial metabolism.[7]

Glycogen synthase kinase-3 (GSK-3) is a serine/threonine protein kinase regulated by phosphorylation, intracellular translocation, and the formation of complexes with other proteins. GSK-3 plays important roles in glycogen metabolism and in cell proliferation, growth, and death.[8-10] There are 2 GSK-3 subtypes, GSK-3α and GSK-3β, and GSK-3β plays a more important role in the heart. Thus, GSK-3β inhibition may be a strategy to limit infarct size upon myocardial reperfusion in pharmacologic and ischemic preconditioning.[11] Such intervention induces GSK-3β phosphorylation at the serine residue 9.[12-14] Furthermore, GSK-3β plays an important role in the nuclear factor erythroid 2-related factor 2 (*Nrf2*) pathway.[15] Nrf2 is a key regulator of several genes, including

South Korea; [f]G.B. Elyakov Pacific Institute of Bioorganic Chemistry, Far-Eastern Branch of the Russian Academy of Science, Vladivostok, Russia; and the [g]Laboratory of Glycoconjugate Chemistry, N.D. Zelinsky Institute of Organic Chemistry, Russian Academy of Sciences, Moscow, Russia. *Drs H. K. Kim, M. Kim, Marquez, and Jeong contributed equally to this work.

The authors attest they are in compliance with human studies committees and animal welfare regulations of the authors' institutions and Food and Drug Administration guidelines, including patient consent where appropriate. For more information, visit the Author Center.

Manuscript received April 1, 2021; revised manuscript received March 31, 2022, accepted May 9, 2022.

JACC: BASIC TO TRANSLATIONAL SCIENCE VOL. 7, NO. 11, 2022
NOVEMBER 2022:1102–1116

NAD(P)H:quinone oxidoreductase 1 (*Nqo1*).[16] Specifically, GSK-3β gene knockdown or inhibition upregulates Nrf2 and its target genes in neuronal cells.[17] However, the role of NPS A in the regulation of cardioprotective mechanisms through the mitochondria remains unknown.

In this study, we examined the clinical potential of NPS A to confer cardioprotection against I/R injury and analyzed its effects on mitochondrial oxidative phosphorylation. We also determined the effects of NPS A on a series of kinases and showed that GSK-3β is a molecular target of NPS A. Docking simulation studies and binding assays revealed that NPS A may bind directly to GSK-3β. Our findings suggest that NPS A regulates the NAD^+/NADH ratio via the Nrf2-Nqo1 pathway.

METHODS

COMPOUNDS. NPS A ($C_{20}H_{18}F_3NO_{10}$; molecular weight = 489 g/mol) (Figure 1A) was isolated from *Neopetrosia* sp and synthesized as previously described.[4] GSK-3β inactivators lithium chloride (LiCl) (Merck) and SB216763 (Sigma-Aldrich) were used to inhibit GSK-3β expression.

ANIMAL EXPERIMENTS. For in vivo treatment of compounds, 3 mg/kg NPS A (dissolved in distilled H_2O), SB216763 (dissolved in dimethyl sulfoxide), or a combination of both SB216763 and NPS A was administered intraperitoneally to 8-week-old C57BL/6 mice every 2 days for a total of 4 weeks.

For the myocardial infarction (MI) model in C57BL/6 mice, 8-week-old mice were anesthetized with 1.5% to 2% isoflurane, and sham and MI procedures were performed according to a published protocol.[18] After MI surgery, mice were injected with 3 mg/kg (bolus, intraperitoneal) NPS A or phosphate-buffered saline every 2 days for 4 weeks. The 3 mg/kg dose was calculated on the basis of the blood volume in mice, which is equivalent to 3.48 μmol/L NPS A (molecular weight = 489 Da). Euthanasia by excision of the heart was performed while mice were under anesthesia; thereafter, the hearts were reserved for subsequent experiments.

All experimental procedures involving animals were performed according to the Guide for the Care and Use of Laboratory Animals, and the protocols were approved by the Institutional Review Board of Animals of the Inje University College of Medicine.

ISOLATION OF RAT HEARTS. The protocol for isolation of 8-week-old rat hearts is described in the Supplemental Appendix.

CELL CULTURE AND SMALL INTERFERING RNA TRANSFECTION. Rat cardiomyoblast H9c2 cells (American Type Culture Collection) were cultured in Dulbecco's modified Eagle's medium with 10% fetal bovine serum, 50 U/mL penicillin, and 50 μg/mL streptomycin (all from Lonza). Lipofectamine 2000 (Thermo Fisher Scientific) was used for small interfering RNA delivery.

MEASUREMENT OF CELL VIABILITY. H9c2 cells were seeded at a density of 2×10^4 cells/well in 96-well culture plates. After 16 hours, the cells were treated with NPS A for 24 hours at doses ranging from 1 to 300 μmol/L. Cell viability was assessed using a 3-[4,5-dimethylthiazol-2-yl]-2,5-diphenyltetrazolium bromide assay kit (Sigma-Aldrich) according to the manufacturer's instructions.

MEASUREMENT OF NAD^+/NADH RATIO. NAD^+/NADH ratio was measured using the NAD^+/NADH-Glo assay (Promega) according to the manufacturer's instructions. Cells were seeded in 96-well culture plates and treated with NPS A after 16 hours. After 1 hour, the assay solution was added, and luminescence was measured using a luminometer (Molecular Device).

MEASUREMENT OF OXYGEN CONSUMPTION RATE. Isolated mitochondria from hearts were analyzed using an XF24 analyzer (Seahorse Bioscience) or an Oroboros Oxygraph-2k system (Oroboros Instruments) for simultaneous measurement of extracellular acidification rate and oxygen consumption rate (OCR) or for measurement of OCR.[19,20] The complete protocol is described in the Supplemental Appendix.

KINASE ASSAY. Kinase assays were performed using the Eurofins KinaseProfiler service according to the protocols detailed by Davies et al.[21] A single dose of NPS A was used during the initial kinase screening assay to identify its target enzymes, resulting in 69 potential candidates. Targets regulated at a minimum of a 20% threshold and statistically significant at a value of $P < 0.05$ were selected.

DOCKING STUDY. AutoDock version 4.01 was used for all docking simulations. The complete protocol is described in the Supplemental Appendix.

WESTERN BLOT. Lysates were centrifuged at 14,000 rpm for 15 minutes at 4°C. A Bradford protein assay (Bio-Rad) was performed following the manufacturer's instructions to determine protein concentrations; then 30 μg protein was loaded per lane onto 10% sodium dodecyl sulfate polyacrylamide gels. Gels were transferred onto nitrocellulose membranes (Whatman) and incubated with specific antibodies (Nqo1 [Abcam]; GSK-3β, phosphorylated GSK-3β [Ser9]

FIGURE 1 NPS A Is Not Toxic in Vitro and in Vivo

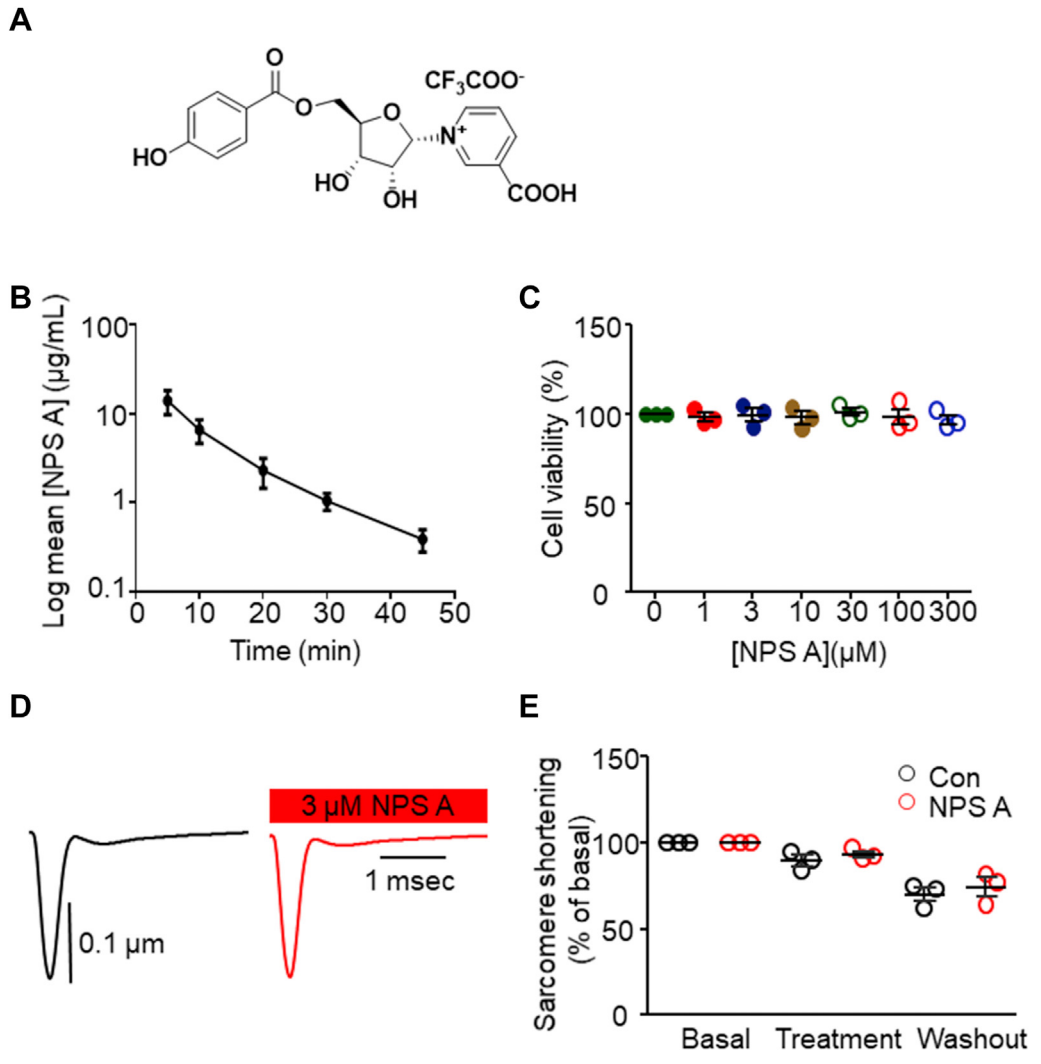

(A) Chemical structure of neopetroside A (NPS A). **(B)** Stability of NPS A in vivo following intravenous administration, measured at the indicated time points. Data represent the average of 3 independent experiments. **(C)** Effects of increasing concentrations (0-300 μmol/L) of NPS A on H9c2 cell viability. Four independent in vitro experiments were performed. **(D, E)** Single-cell contractility assay in the presence and absence of 3 μmol/L NPS A. Data represent the average of 3 independent experiments. Data were analyzed using 1-way analysis of variance followed by the Bonferroni multiple-comparisons test **(C)** and Student's *t*-test **(D)**.

[Cell Signaling]; and glyceraldehyde-3-phosphate dehydrogenase [Santa Cruz Biotechnology]). Protein bands were detected by western blot using AbSignal (AbClon) and a LAS-3000 Plus imager (Fuji Photo Film).

SURFACE PLASMON RESONANCE BINDING ASSAY. Direct target binding of free NPS A was assessed using a dual-channel surface plasmon resonance instrument (Biacore T200, Cytiva). The complete protocol is described in the Supplemental Appendix.

ISOLATION OF CARDIOMYOCYTES AND FLUORESCENCE STAINING. Hearts of 8-week-old male C57BL/6 mice were perfused with normal Tyrode's solution with collagenase on a Langendorff system to obtain single cardiomyocytes.[22] Isolated cardiomyocytes were incubated with 10 μmol/L CM-H2DCFDA (General Oxidative Stress Indicator, Thermo Fisher Scientific) for 30 minutes. The resulting fluorescence intensity was detected using an LSM-800 confocal microscope (Carl Zeiss).

FIGURE 2 **NPS A Elevates Glycolysis, OCR, and Metabolic Processes in Rat Cardiomyoblast H9c2 Cells**

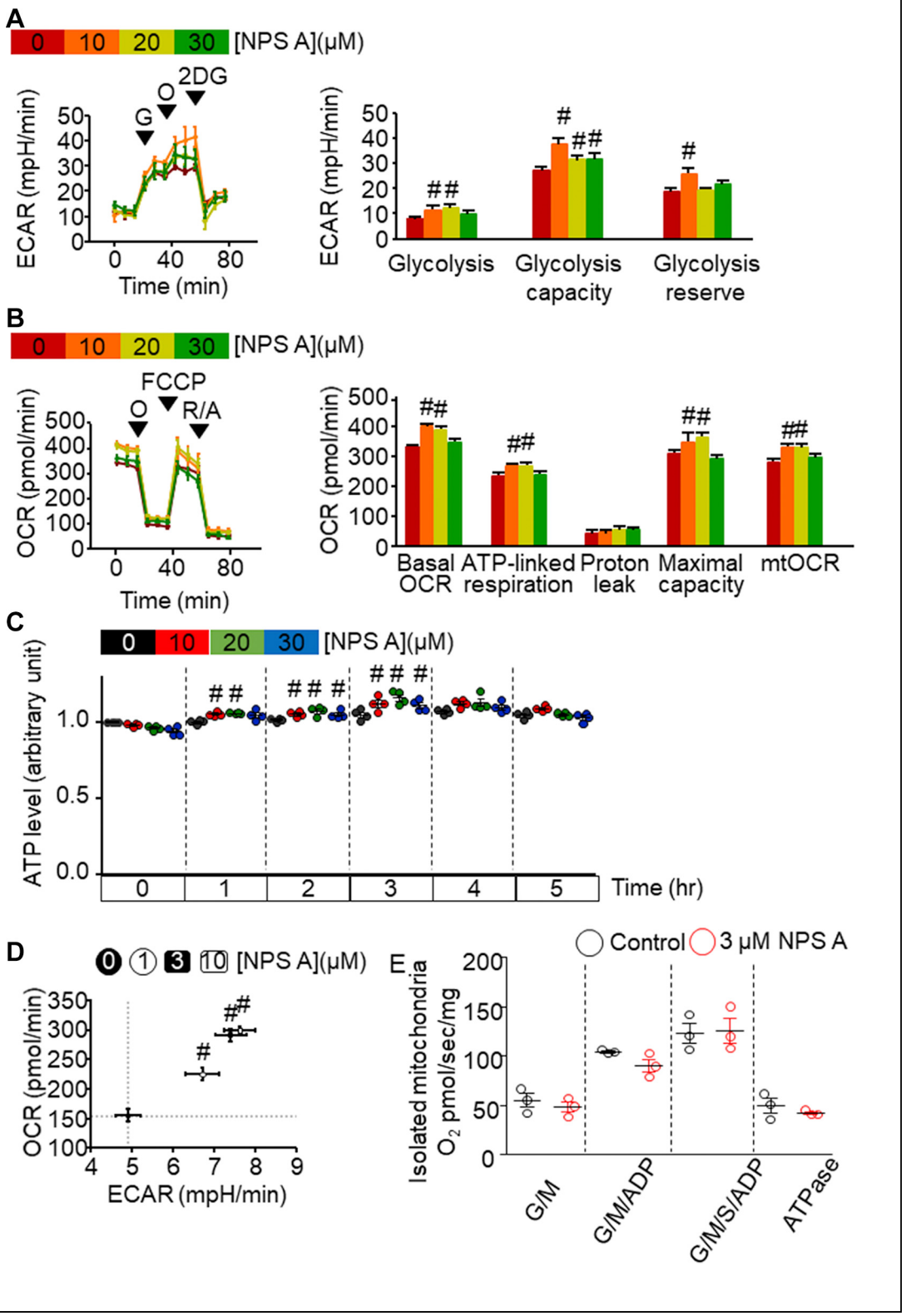

Continued on the next page

HISTOLOGIC ANALYSES. Mouse hearts were excised, washed with phosphate-buffered saline, and fixed in 10% paraformaldehyde. For assessment of myocardial fibrosis, sections were sent to Histoire for Masson's trichrome collagen staining. Sections were photographed using a NanoZoomer Digital Slide Scanner (Hamamatsu Photonics). The relative fibrotic area (percentage of total area) was measured quantitatively using ImageJ version 1.48.

SIMULATED I/R INJURY. Simulated I/R was initiated in cardiac cell lines or isolated mouse ventricular myocytes, as previously described.[22,23] The complete buffer composition and protocol are described in the Supplemental Appendix.

STATISTICAL ANALYSIS. Data are presented as mean ± SEM. Differences between 2 groups were analyzed using unpaired 2-tailed Student's *t*-tests. Differences between more than 2 groups were analyzed using 1- or 2-way analysis of variance followed by Bonferroni post hoc tests for multiple pairwise comparisons. Statistical significance was set at $P < 0.05$. The log-rank Mantel-Cox test was performed to compare survival among the groups. Analyses were performed using Origin version 8.0 (OriginLab) and Prism version 9.0 (GraphPad Software).

RESULTS

NPS A IS NONTOXIC IN VIVO AND IN VITRO. In the investigation of in vivo stability (Figure 1A), administration of synthesized NPS A (6 mg/kg) resulted in undetectable NPS A levels in the blood (data not shown). When administered intraperitoneally at 3 mg/kg, NPS A was detected in the circulation but rapidly decreased to 10% of its initial concentration within 30 minutes (Figure 1B). In the cellular H9c2 model, NPS A did not exhibit any toxic effects at doses ≤300 μmol/L (Figure 1C). In the examination of electric stimulation–induced sarcomere shortening in single cardiac myocytes, treatment with NPS A did not affect the single-cell contractility (Figures 1D and 1E).

NPS A INCREASES GLYCOLYSIS, OXIDATIVE PHOSPHORYLATION, AND ATP PRODUCTION IN VITRO. We then examined whether NPS A treatment enhances glycolysis. As measured by extracellular acidification rate, cells treated with 10 μmol/L NPS A exhibited the greatest increases in glycolysis, glycolytic capacity, and glycolytic reserve (Figure 2A). We next measured changes in OCR after NPS A treatment. Compared with control, treatment with 10 or 20 μmol/L NPS A enhanced mitochondrial function, such as ATP-linked respiration and mitochondrial OCR and increased mitochondrial oxygen maximal capacity (Figure 2B). Furthermore, NPS A treatment caused cellular ATP levels to be elevated for 3 hours before returning to baseline levels (Figure 2C).

Treatment with lower concentrations (3 and 10 μmol/L) of NPS A resulted in similarly high OCR and extracellular acidification rate (Figure 2D, Supplemental Figures 1B to 1D), without affecting mitochondrial membrane potential (Supplemental Figure 1A). However, in isolated mitochondria, we observed no difference in OCR between the untreated and 3 μmol/L NPS A–treated groups (Figure 2E). These data indicate that NPS A treatment enhances glycolysis and oxidative phosphorylation, causing the transient up-regulation of energy metabolism rather than directly affecting mitochondrial function.

NPS A AMELIORATES I/R INJURY EX VIVO. In the ex vivo Langendorff-perfused system experiment, impaired left ventricular pressure and heart function were mitigated by NPS A treatment after I/R treatment (Figures 3A and 3B). The mean left ventricular developed pressure and maximum dP/dt after 30 minutes of reperfusion were significantly lower in the

FIGURE 2 Continued

(A) Left: Extracellular acidification rate (ECAR) output of H9c2 cells and response to 10 mmol/L glucose (G), 1 μmol/L oligomycin (O), and 10 mmol/L 2-deoxyglucose (2DG). **Right:** Effects of increasing concentrations of neopetroside A (NPS A) on glycolysis, glycolytic capacity, and glycolytic reserve on the basis of data derived from the **left panel**. Four independent in vitro experiments were performed. #$P < 0.05$ vs control cells. **(B) Left:** Representative graph of oxygen consumption rate (OCR) of H9c2 cells in response to 1 μmol/L O, 1 μmol/L carbonyl cyanide-4-(trifluoromethoxy)phenylhydrazone (FCCP), and 1 μmol/L rotenone with 1 μmol/L antimycin (R/A). **Right:** Effects of increasing concentrations of NPS A on mitochondrial function parameters (adenosine triphosphate [ATP]-linked respiration, proton leakage, mitochondrial oxygen maximal capacity, and mitochondrial OCR [mtOCR]) on the basis of data derived from the **left panel**. Four independent in vitro experiments were performed. #$P < 0.05$ vs control cells. **(C)** ATP levels after treatment with NPS A for the indicated times. Data represent the average of 4 independent experiments. **(D)** OCR (y-axis) against ECAR (x-axis) according to concentration of NPS A. Four independent in vitro experiments were performed. #$P < 0.05$ vs control cells. **(E)** OCR measurement in isolated cardiac mitochondria. Three independent in vitro experiments were performed. Data were analyzed using 1-way analysis of variance followed by the Bonferroni multiple-comparisons test **(A to D)** and Student's *t*-test **(E)**. ADP = adenosine diphosphate; ATPase = adenosine triphosphatase; G/M = glutamate-maleate; S = succinate.

FIGURE 3 NPS A Preserves Decreased LVDP After Global I/R Injury

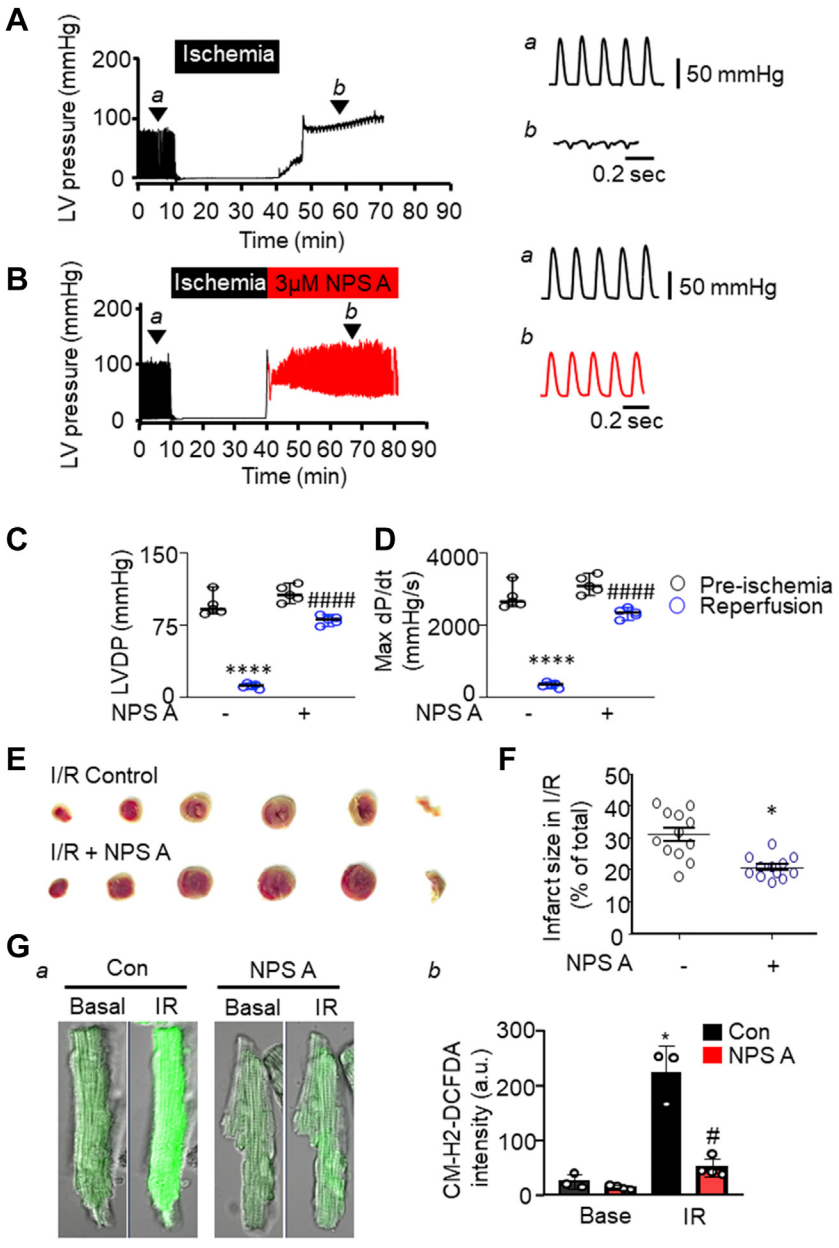

(A, B) Representative recordings of left ventricular (LV) pressure in perfused hearts without **(A)** or with **(B)** 3 μmol/L neopetroside A (NPS A) treatment following ischemia. **(C, D)** LV developed pressure (LVDP) and maximum dP/dt were determined before ischemia and during reperfusion in the presence and absence of NPS A. n = 5 per group. ****$P < 0.0001$ vs preischemia in the control, and ###$P < 0.001$ vs reperfusion in the control. **(E, F)** Representative photographs and quantitative analysis of rat hearts comparing infarct sizes in animals with and without NPS A treatment after ischemia/reperfusion (I/R) injury. n = 6 per group. Evaluated points for I/R: n = 12 in each group. *$P <$ 0.05 vs non-NPS A-treated control. **(G)** Representative images and quantitative analysis of nontreated and NPS A-treated isolated cardiomyocytes stained with CM-H2-DCFDA during basal conditions or after I/R injury. Control n = 3, I/R n = 4 per group. *$P < 0.05$ vs preischemia in the control, and #$P < 0.05$ vs reperfusion in the control. In **A, B, and G, a and b** are zoomed images of the recordings from the representative Figures. Data were analyzed using 2-way analysis of variance followed by the Bonferroni multiple-comparisons test **(C, D, Gb)** and Student's *t*-test **(F)**.

hearts treated with NPS A than in the preischemia group (Figures 3C and 3D). Moreover, NPS A-treated hearts exhibited significantly smaller infarct size and lower reactive oxygen species levels than untreated I/R hearts (Figures 3E to 3G). These findings suggest that NPS A reduces infarct formation after global I/R injury by preserving hemodynamic status and mitochondrial respiration capacity and by suppressing reactive oxygen species generation.

NPS A REDUCES INFARCTION IN VIVO TO INCREASE SURVIVAL RATE. Next, we investigated whether NPS A prevents MI in vivo (Figure 4A). The survival rate of MI control mice was 53% (8 of 15) at the end of the experiment, whereas mice treated with NPS A exhibited a survival rate of 80% (12 of 15). The sham group exhibited 100% survival (15 of 15) (Figure 4B). The survival curves of the groups were significantly different ($P = 0.011$).

NPS A-treated mice showed a distinct reduction in infarction at 3 weeks post-MI (Figure 4C). Detailed histologic analysis of Masson's trichrome staining of heart longitudinal and cross sections showed that NPS A treatment reduced MI (Figure 4D). NPS A treatment during MI did not increase heart weight indexed to body weight or heart weight indexed to tibia length, indicating that NPS A did not protect against cardiac hypertrophy (Figures 4E and 4F, Supplemental Figure 2A). However, NPS A treatment decreased the expression of fibrotic markers collagen type I alpha 1 chain and α-smooth muscle actin compared with that in MI. (Supplemental Figure 2B). Overall, our results showed that NPS A confers cardioprotection against MI in vivo by decreasing the infarct area (Figure 4G).

NPS A INHIBITS GSK-3β ACTIVITY. We then screened energy metabolism pathways targeted by NPS A using in vitro kinase activity assays. Among the 69 kinases identified in the presence of NPS A, NPS A treatment was associated with reduced kinase activity of GSK-3β and mammalian target of rapamycin (mTOR) (Figure 5A). To determine the half maximal inhibitory concentration of NPS A, we measured the kinase activity of GSK-3β and mTOR after NPS A treatment at different doses. NPS A exhibited a half maximal inhibitory concentration of 121 μmol/L against GSK-3β (Figure 5B); however, the kinase activity of mTOR did not respond to increasing doses of NPS A (Figure 5C). The mTOR inhibitory effect of NPS A shown in kinase screening was therefore considered a pseudo-effect.

NPS A DIRECTLY BINDS WITH GSK-3β. To elucidate the possible mechanism of interaction between NPS A and GSK-3β, we performed molecular docking simulations using AutoDock version 4.01.[24] Among the various GSK-3β complexes in the Protein Data Bank, we selected 1Q4L because its small-molecule ligand is similar to NPS A, with 2 aromatic rings, 1 of which has a carboxylic acid function (inhibitor I-5). First, we simulated the docking of inhibitor I-5 to its binding site. After 60 runs, we found a cluster containing 44 conformations, from which the lowest binding energy was −9.6 kcal/mol. The average root mean square deviation in Cartesian coordinates from the starting structure was approximately 1.0 Å. Using isothermal titration calorimetry, the experimental free energy of binding was previously measured at −9.7 kcal/mol.[25] In docking simulations for NPS A and its β-isomer, 60 runs produced 2 major clusters with a total of 29 conformations. Both clusters suggested contact between the carboxylic group of NPS A and Arg141 of GSK-3β but differed in the orientation of the *p*-hydroxybenzoyl substituent within the binding site. The lowest binding energy for this interaction was −9.4 kcal/mol.

Given that NPS A shares a similarity with the structure of I-5, we also performed docking simulations to determine possible binding behavior. Our results indicated that NPS A may bind to GSK-3β, similar to inhibitor I-5. Both NPS A and I-5 exhibited interactions with Arg141, Val135, and Tyr134 (Figure 5D, Supplemental Figures 3A to 3C).

In surface plasmon resonance binding assays with GSK-3β and increasing concentrations of NPS A, a general increase in binding signal was observed with increasing NPS A. Calculation of the dissociation constant K_D indicated direct binding of NPS A with GSK-3β at 92.4 μmol/L (Figure 5E).

NPS A INCREASES NAD^+/NADH RATIO THROUGH THE GSK-3β/Nrf2/Nqo1 AXIS. NPS A treatment in vitro was associated with significantly increased NAD^+/NADH ratios at concentrations of 3 and 10 μmol/L (Supplemental Figure 4A). Application of the known GSK-3β inhibitor SB216763 resulted in a dose-dependent increase of the NAD^+/NADH ratio in the treated cells, with a 10 μmol/L dose resulting in a significant ratio increase (Supplemental Figure 4B).

NPS A had no effect on GSK-3β phosphorylation at Ser9 or Tyr216 in vitro. (Supplemental Figure 5A). We also observed that GSK-3β phosphorylation was unchanged during NPS A treatment in vivo. Additionally, the downstream targets β-catenin, Nrf2, and Nqo1 significantly increased in all treatment groups in both in vitro and in vivo models (Figures 6A and 6B, Supplemental Figures 5B and 5C).

To examine whether the observed increase in the NAD^+/NADH ratio was dependent on the Nrf2-Nqo1 pathway, we treated cells with small interfering RNA against *Nrf2* or *Nqo1* (Supplemental

FIGURE 4 NPS A Protects Against MI

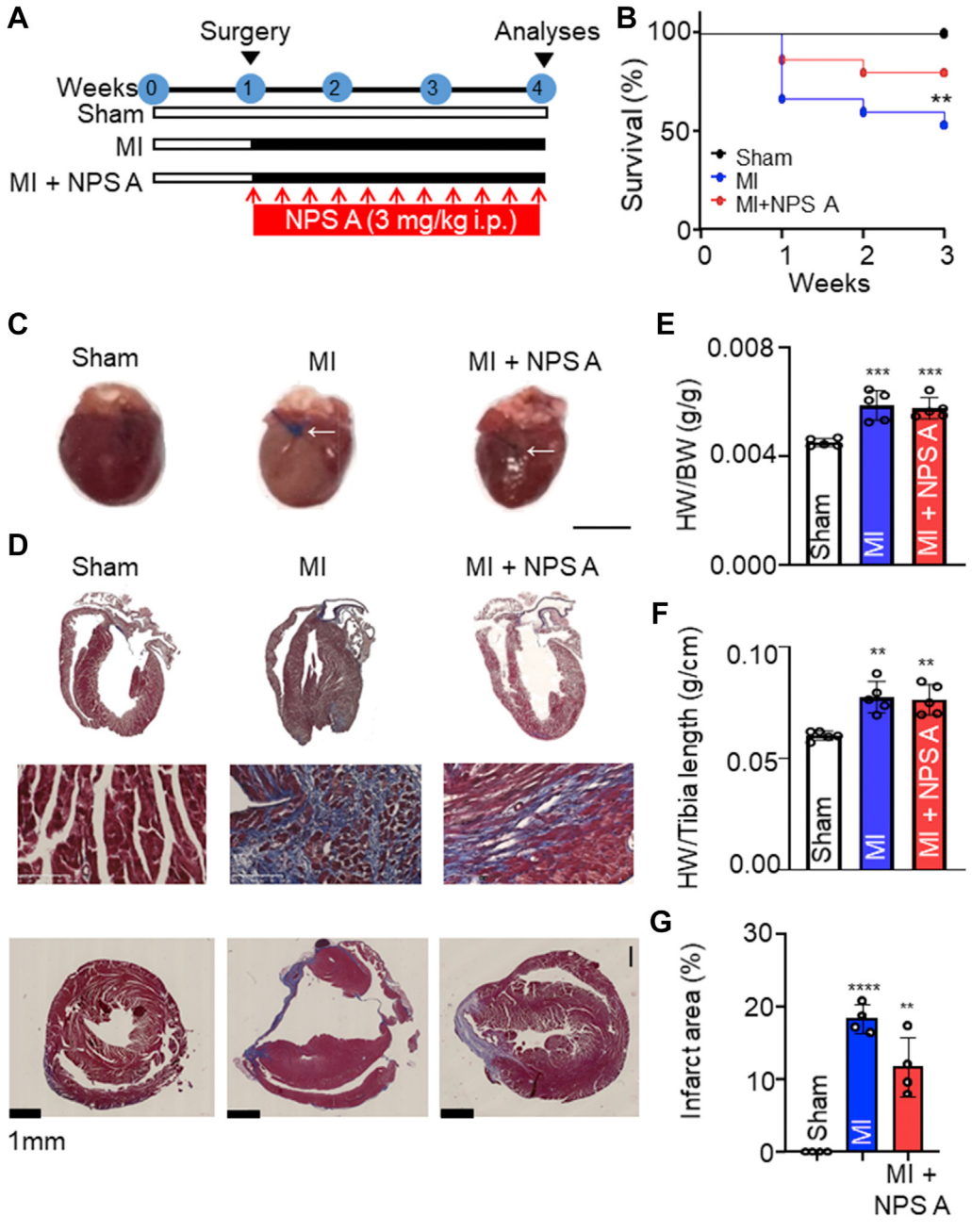

(A) In vivo protocol of the 4-week myocardial infarction (MI) model in 8-week-old C57BL/6 mice. **Arrows** indicate intraperitoneal (i.p.) injection. **(B)** Survival rates of model animals. Start of the analysis, n = 15 mice per group. $^{**}P < 0.01$ vs sham group. **(C)** Representative heart morphology after MI surgery. **Arrows** indicate coronary occlusion. **(D)** Representative photograph of Masson's trichrome-stained mouse heart (**top 2 rows**, longitudinal section; **bottom 2 rows**, cross section; longitudinal section: **black scale bar** = 5 mm, **white scale bar** = 40 μm; cross section, **black scale bar** = 1 mm, **white scale bar** = 100 μm). **(E)** Heart weight (HW)/body weight (BW) and **(F)** HW/tibia length ratios after sham, MI, and MI plus neopetroside A (NPS A) treatment. n = 5 mice in each group. $^{**}P < 0.01$, $^{***}P < 0.001$, and $^{****}P < 0.0001$ vs sham group. **(G)** Infarct analysis of infarct area on the basis of Figure 3D. n = 4 mice in each group. $^{**}P < 0.01$ and $^{****}P < 0.0001$ vs sham group. Data were analyzed using 1-way analysis of variance followed by the Bonferroni multiple-comparisons test **(E to G)**.

FIGURE 5 NPS A Inhibits GSK-3β Kinase Activity in Vitro and Interacts With GSK-3β in Molecular Docking Simulations

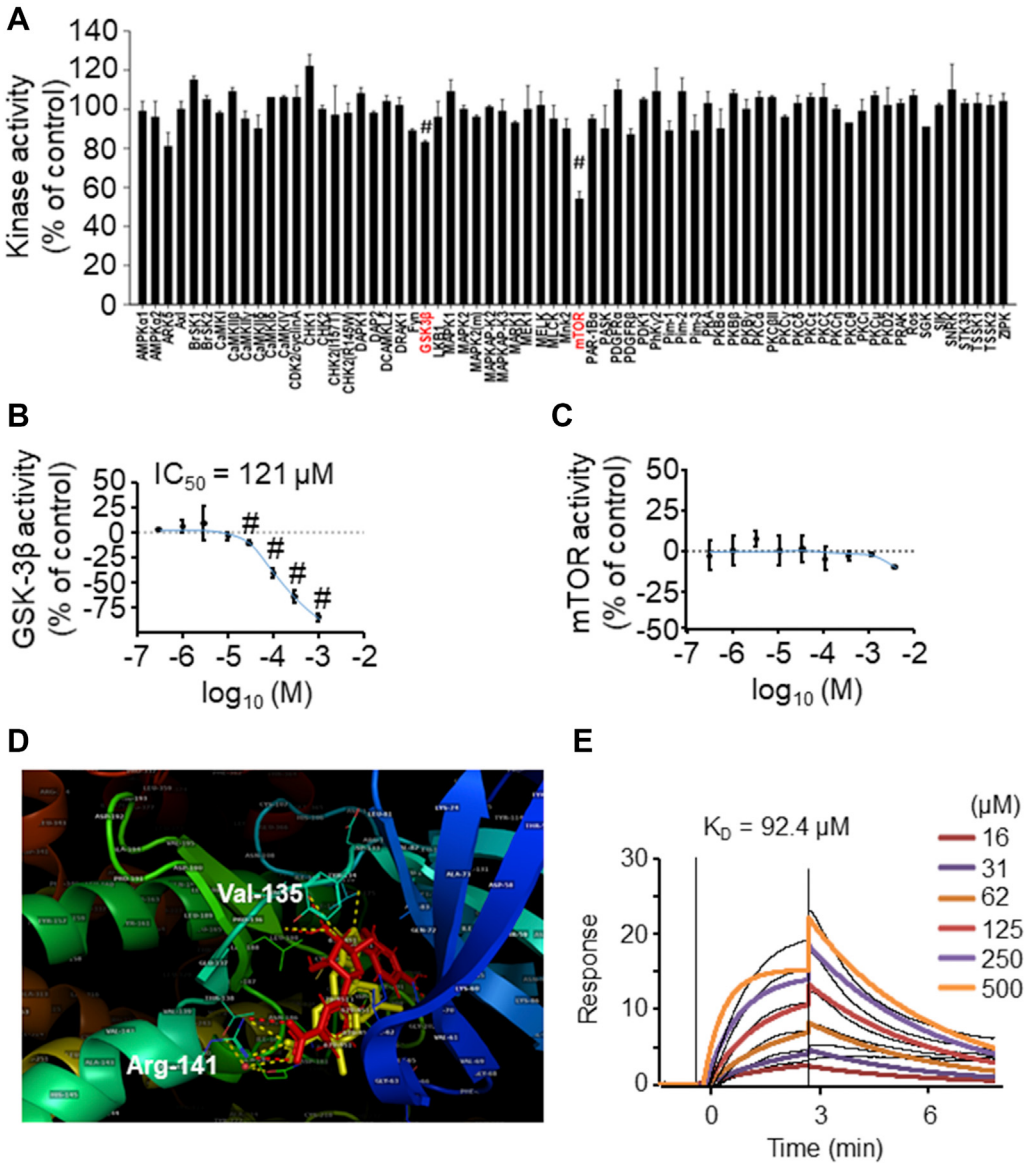

(A) An in vitro kinase activity screen was performed to determine which kinases were modulated by neopetroside A (NPS A). Three independent in vitro experiments were performed. #$P < 0.05$ vs control. **(B, C)** Inhibitory activities of increasing concentrations of NPS A on glycogen synthase kinase-3β (GSK-3β) and mammalian target of rapamycin (mTOR), with half maximal inhibitory concentration (IC_{50}) values. Three independent in vitro experiments were performed. #$P < 0.05$ vs control. **(D)** Overlay of the docked NPS A conformation **(red)** and the crystallographic conformation of I-5 **(yellow)**. Corresponding interactions with GSK-3β are shown in **red** and **yellow dashes**, respectively. **(E)** Surface plasmon resonance (SPR) binding assay for NPS A and GSK-3β. Data were analyzed using 1-way analysis of variance followed by the Bonferroni multiple-comparisons test **(A)**.

Figures 6A and 6B). Compared with SB216763, NPS A treatment led to a greater ratio increase. Moreover, down-regulation of both *Nrf2* and *Nqo1* abolished the NPS A-induced increase in the NAD^+/NADH ratio but did not affect the SB216763-induced increase as considerably (**Figure 6C**). NPS A and SB216763 cotreatment induced a higher NAD^+/NADH ratio than NPS A treatment alone, suggesting that GSK-3β inhibitors exerted additive effects on the NAD^+/NADH ratio (**Figure 6D**). Our data suggest that the inhibition

FIGURE 6 NPS A Increases the NAD$^+$/NADH Ratio Through the Nrf2/Nqo1 Pathway In H9c2 Cells

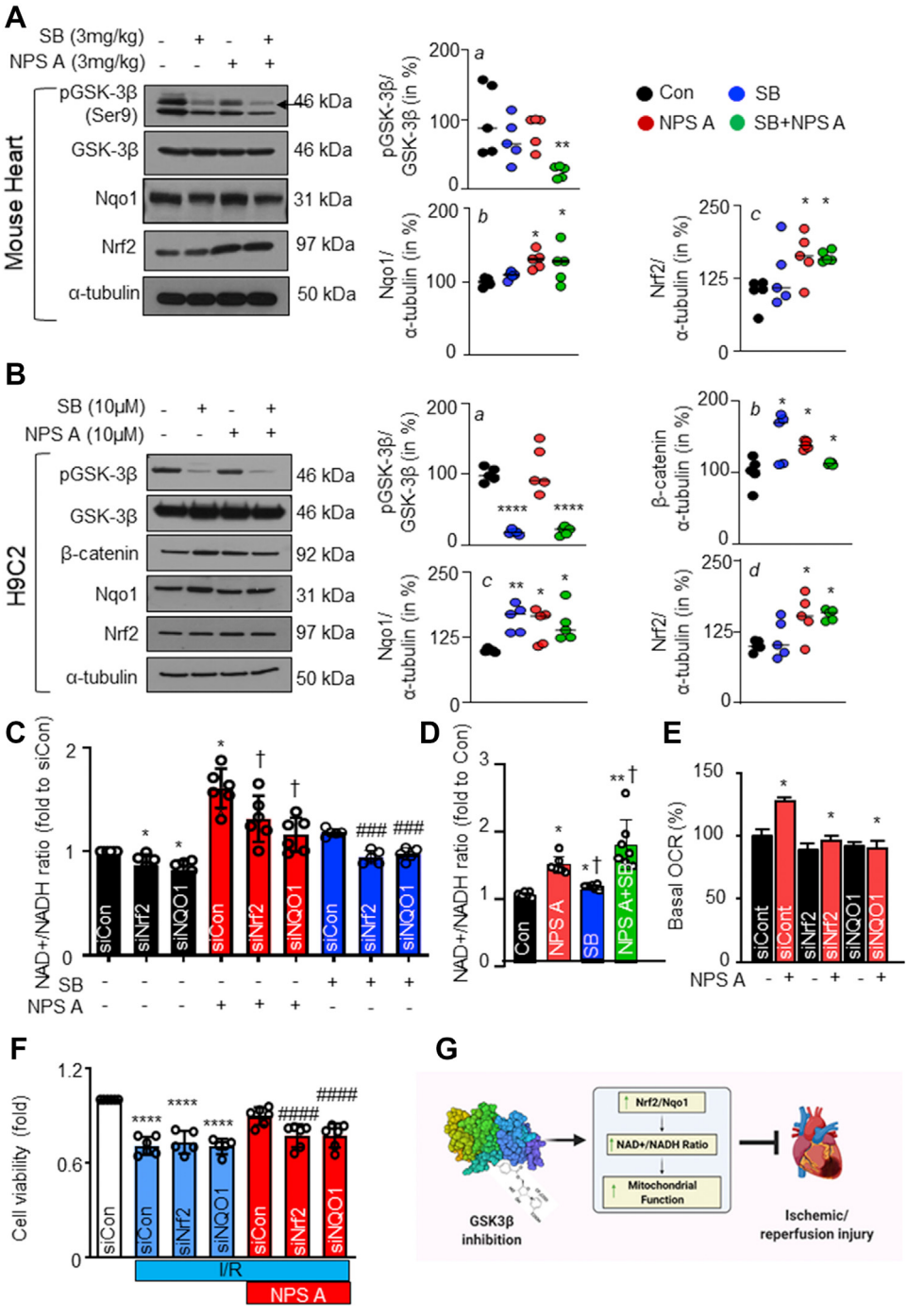

Continued on the next page

of GSK-3β contributed to changes in the NAD$^+$/NADH ratio.

Upon examining the effect of GSK-3β downstream gene inhibition, we found that OCR was increased by NPS A treatment and decreased by knockdown of *Nrf2* or *Nqo1* in the presence of NPS A (Figure 6E). To examine whether the cardioprotective effects of NPS A are mediated by Nrf2 or Nqo1, the cells were exposed to

simulated I/R conditions in the presence of NPS A, *Nrf2*, or *Nqo1* small interfering RNA. NPS A conferred cardioprotection during simulated I/R, and this effect was abolished by knockdown of *Nrf2* or *Nqo1*. Knockdown of *Nrf2* and *Nqo1* during simulated I/R NPS A treatment resulted in viability levels similar to those observed during *Nrf2*/*Nqo1* knockdown during simulated I/R only. The levels in *Nrf2*/*Nqo1* knockdown during simulated I/R only represented the maximal damage I/R can confer on the cells, and knockdown of *Nrf2* or *Nqo1* did not confer any additional damage. Overall, the results indicate that NPS A targeted the Nrf2/Nqo1 axis to confer cardioprotection in cells after I/R injury through a GSK-3β phosphorylation-independent mechanism (**Figure 6F**).

DISCUSSION

Our findings demonstrate that NPS A exerted antifibrotic and cardioprotective effects against acute I/R injury and in MI conditions by improving cardiac hemodynamic status and mitochondrial respiration capacity. NPS A increased mitochondrial oxidative phosphorylation and ATP production in the treated cardiac cell line but did not directly increase mitochondrial oxygen consumption in the isolated mitochondria, suggesting that the increased mitochondrial function occurred via changes to intracellular signaling pathways. The phosphorylation-independent inhibition of GSK-3β regulated the NAD^+/NADH ratio by activating Nrf2/Nqo1 to improve cellular and mitochondrial functions.

Using an in vitro cell-free kinase screening assay, molecular binding simulation studies, and surface plasmon resonance analysis, we identified GSK-3β as a direct molecular target of NPS A. GSK-3α and GSK-3β have similar biochemical properties and substrate recognition, but the 2 are not always functionally identical or interchangeable.[26] Although the cardioprotective effect of GSK-3β is well reported, recent studies have also demonstrated that GSK-3α plays an important role in aging hearts and in different heart failure models, including pressure overload, lipotoxic cardiomyopathy, and MI.[27-32] Some proposed cardioprotective mechanisms of GSK-3α inhibition include mTOR inhibition, mitochondrial permeability transition pore (mPTP) opening, or peroxisome proliferator-activated receptor α-mediated lipotoxicity.[28-30] However, findings on the role of GSK-3α remain contradictory. For example, rapid deterioration of the heart and its cardiac parameters was noted in GSK-3$\alpha^{-/-}$ mice, but GSK-3α deficiency also induced cardiac hypertrophy and contractile dysfunction in an aging mouse model.[28,32] These findings suggest the diverse responses and pathophysiological roles of GSK-3α in various disease states.

Although GSK-3α may be involved in the NPS A-induced cardioprotective mechanism, the results of the present study demonstrate that its effect is exerted by GSK-3β inhibition through the Nrf2/Nqo1 axis to regulate the NAD^+/NADH ratio. Furthermore, NPS A did not affect mTOR activity (**Figure 5C**) and mPTP opening (Supplemental Figure 7). There have been no studies demonstrating a relationship between GSK-3α inhibition and NAD^+/NADH regulation through the Nrf2/Nqo1 mechanism; nonetheless, our present findings provide strong evidence that NPS A-induced inhibition of GSK-3β has cardioprotective effects rather than GSK-3α inhibitory effects. Future studies should study the inhibitory effect of NPS A on GSK-3α and how this can regulate cardiac function and downstream signaling to confer cardioprotection in a heart failure model. Furthermore, obesity-induced lipotoxicity is a different experimental model, and thus the mechanisms involved are outside of the scope of the present study.

FIGURE 6 Continued

(A, B) In vivo and in vitro representative western blots of neopetroside A (NPS A) and SB216763-treated C57BL/6 mice and H9c2 cells, respectively, and their respective quantitative analysis. In vivo **(A)**: n = 5, all groups. In vitro **(B)**: 5 independent in vitro experiments were performed. *$P < 0.05$ vs control and **$P < 0.01$ vs control. **(C)** Nicotinamide adenine dinucleotide (NAD^+)/nicotinamide adenine dinucleotide, reduced (NADH) levels as determined with control, nuclear factor erythroid 2-related factor 2 (*Nrf2*), or NAD(P)H quinone oxidoreductase 1 (*Nqo1*) small interfering RNA (siRNA) treatment in the presence or absence of 10 μmol/L NPS A or SB216763. Four independent in vitro experiments were performed. *$P < 0.05$ vs control, †$P < 0.05$ vs siCon + NPS A, and ###$P < 0.001$ vs siCon + SB216763. **(D)** Measurement of NAD^+/NADH ratio after treatment with SB216763 and/or NPS A. Six independent in vitro experiments were performed. *$P < 0.05$ vs control, **$P < 0.01$ vs control, and †$P < 0.05$ vs NPS A. **(E)** Basal oxygen consumption rate (OCR) in H9c2 cells following treatment with control, *Nrf2*, or *Nqo1* siRNA in the presence or absence of NPS A. Four independent in vitro experiments were performed. *$P < 0.05$ vs respective controls. **(F)** Cell viability after simulated ischemia/reperfusion (sI/R) injury in cells treated with control, *Nrf2*, or *Nqo1* siRNA in the presence or absence of NPS A. Five independent in vitro experiments were performed. ****$P < 0.0001$ vs siCon and ####$P < 0.0001$ vs sI/R with NPS A treatment. **(G)** Proposed mechanism of the protective role of NPS A in I/R injury. Created with BioRender.com. Data were analyzed using 1-way analysis of variance (ANOVA) followed by the Bonferroni multiple-comparisons test **(A, B, D)**, 2-way ANOVA followed by the Bonferroni multiple-comparisons test **(C, F)**, and Student's *t*-test **(E)**.

The action of NPS A on GSK-3β is of special interest, as GSK-3β is a protein kinase that participates in the pathogenesis of hypertrophy, fibrosis, heart failure,[14,33,34] and I/R injury. Moreover, ischemic preconditioning induces phosphorylation and inhibition of GSK-3β, and its pharmacologic inhibition mimics the cardioprotective effects of preconditioning.[14,35] Pharmacologic inhibition of GSK-3β protects against I/R-induced damage in the heart, and as a result, inhibitors of GSK-3β have been investigated both for therapeutic use and to better understand how GSK-3β activity is regulated in the heart.

GSK-3β inhibition prevents the opening of mPTPs under oxidative stress conditions.[36] GSK-3β inhibition decreases the binding of cyclophilin D to adenine nucleotide translocase, which significantly reduces the opening threshold of mPTP.[26] NPS A treatment did not prevent Ca^{2+}-induced mPTP opening, which indicates that NPS A-induced GSK-3β inhibition confers cardioprotection through an mPTP-independent mechanism (Supplemental Figures 7A and 7B). Inhibition of GSK-3β may also confer cardioprotection through the reduction of oxidative stress under I/R conditions. Known GSK-3β inhibitors, such as LiCl and inhibitor II, can reduce mitochondrial reactive oxygen species production by targeting mitochondrial complexes and Rieske subunits.[36] Another GSK-3β inhibitor, SB216763, reduces I/R-induced reactive oxygen species generation and mPTP opening in an age-dependent manner in rat hearts.[37]

GSK-3β activity is regulated by phosphorylation or competitive inhibition at its ATP-binding site.[25] The effect of NPS A appears to have a mechanism different from that of conventional GSK-3β inhibitors in that it is independent of GSK-3β phosphorylation regulation.[38] We found that NPS A inhibited GSK-3β activity via direct binding, similar to the ATP mimetic competitive inhibitor I-5.[35] Previous studies have reported that Arg141 interacts with the I-5 carboxylate group in the GSK-3β/I-5 complex, in which the side chains of Arg141 rotate to interact with the carboxylate oxygen atoms of the inhibitor.[25] This type of interaction may serve as a mechanism underlying the observed NPS A action.

Our results are the first to demonstrate the regulation of NAD^+/NADH ratios in the heart through a GSK-3β-related mechanism, which was previously observed only in the brain.[39] We have demonstrated that NPS A exerts its effect on metabolic processes by altering the NAD^+/NADH ratio in cardiomyocytes. Furthermore, the NPS A-induced increase in the NAD^+/NADH ratio is likely a cause, rather than a consequence, of mitochondrial function preservation. Cellular NAD^+/NADH ratio determines the oxidative capacity of cells, controls the activities of key cellular respiration enzymes, and can confer protection against cardiotoxins. Generally, NAD^+ homeostasis is reduced in heart failure models. Studies have suggested that the NAD pool is related to cardiac remodeling and mitochondrial dysfunction in the heart, and targeting intracellular NAD^+ is a possible intervention strategy to address cardiac dysfunction.[40,41] Stimulating NAD^+ to restore and preserve cardiac function has been successful in recent studies. NAD biosynthesis is commonly stimulated through the use of NAD^+ precursors, which are sourced mainly from vitamin B_3 nicotinamide and nicotinamide riboside.[42] The supplemental use of these precursors has been shown to stabilize myocardial NAD^+ levels in the failing heart and inhibit the progression of heart failure by restoring cardiac bioenergetics.[43,44]

We also demonstrated that the up-regulation of the Nrf2/Nqo1 axis is responsible for increasing NAD^+/NADH ratio by NPS A-induced GSK-3β inhibition. GSK-3β activates Nrf2 degradation and inhibits its downstream target, *Nqo1*.[45] Nqo1 itself is known to augment NAD^+ levels and confers protection against cardiotoxins.[46] In addition, GSK-3β inhibition using LiCl was found to activate Nrf2 and protect against ventricular arrhythmias,[47] further strengthening our hypothesis regarding the inhibitory effect of NPS A on GSK-3β. β-catenin, a known mediator of fibrosis through phosphorylated GSK-3β,[48] also contributed to this regulation, considering that the NAD^+/NADH ratio was observed to be decreased in the ethanol intoxication model of β-catenin deficiency.[49]

STUDY LIMITATIONS. The current study has several limitations that need to be addressed. First, our study only performed analysis on I/R and MI models. Considering heart failure is a multi-step, multi-factorial disease, the effects of NPS A on other in vivo models of cardiovascular disease and heart failure should be performed. Second, the exact mechanism how NPS A induces a phosphorylation-independent mechanism still needs to be determined. Third, although the results of the current study have established that the inhibitory effects of NPS A on GSK-3β courses through the Nrf2/Nqo1 axis, detailed analysis on the inhibitory effect of GSK-3α and related downstream proteins and how this can regulate cardiac function to confer cardioprotection should also be considered.

CONCLUSIONS

In summary, our findings suggest that the novel pyridine nucleoside NPS A enhances mitochondrial function and protects tissue integrity after I/R-induced cardiac damage, presumably via modulation of GSK-3β activity. This effect is mediated by the up-regulation of the NAD^+/NADH ratio via activation of the GSK-3β/Nrf2/Nqo1 signaling axis (**Figure 6G**). Although the precise mechanism by which NPS A induces phosphorylation-independent regulation of GSK-3β has not yet been elucidated, the pharmacologic effects of NPS A differ from those of existing phosphorylation-based GSK-3β inhibitors, providing important information for the development of drugs to treat cardiovascular injury.

FUNDING SUPPORT AND AUTHOR DISCLOSURES

This work was supported by the Basic Science Research Program (NRF-2020R1A4A1018943 and NRF-2018R1A2A3074998) through the National Research Foundation of Korea, funded by the Ministry of Education and the Ministry of Science and ICT. The synthesis of NPS A was supported by the Russian Science Foundation (grant 19-73-30017). The authors have reported that they have no relationships relevant to the contents of this paper to disclose.

ADDRESS FOR CORRESPONDENCE: Dr Jin Han, National Research Laboratory for Mitochondrial Signaling, Department of Physiology, College of Medicine, Cardiovascular and Metabolic Disease Center, Inje University, Busan 47393, South Korea. E-mail: phyhanj@inje.ac.kr.

PERSPECTIVES

COMPETENCY IN MEDICAL KNOWLEDGE: GSK-3β is fundamental in cardiac development and in the pathogenesis of hypertrophy, fibrosis, heart failure, and I/R injury. Pharmacologic inhibition of GSK-3β confers protection against various heart pathologies and thus has been an attractive avenue for cardiac therapeutics.

TRANSLATIONAL OUTLOOK: NPS A treatment is an effective pharmacologic intervention strategy for protecting the human heart against acute I/R damage and myocardial fibrosis in the treatment or prevention of heart failure. These findings are essential for the future development of GSK-3β-targeting drugs for cardiac medicine.

REFERENCES

1. Handy DE, Loscalzo J. Redox regulation of mitochondrial function. *Antioxid Redox Signal*. 2012;16:1323–1367.

2. Brown DA, Perry JB, Allen ME, et al. Expert consensus document: mitochondrial function as a therapeutic target in heart failure. *Nat Rev Cardiol*. 2017;14:238–250.

3. Oku N, Matsunaga S, van Soest RW, Fusetani N. Renieramycin J, a highly cytotoxic tetrahydroisoquinoline alkaloid, from a marine sponge *Neopetrosia* sp. *J Nat Prod*. 2003;66:1136–1139.

4. Shubina LK, Makarieva TN, Yashunsky DV, et al. Pyridine nucleosides neopetrosides A and B from a marine *Neopetrosia* sp. sponge. Synthesis of neopetroside A and its beta-riboside analogue. *J Nat Prod*. 2015;78:1383–1389.

5. Ussher JR, Jaswal JS, Lopaschuk GD. Pyridine nucleotide regulation of cardiac intermediary metabolism. *Circ Res*. 2012;111:628–641.

6. Stein LR, Imai S. The dynamic regulation of NAD metabolism in mitochondria. *Trends Endocrinol Metab*. 2012;23:420–428.

7. Ying W. NAD^+/NADH and $NADP^+$/NADPH in cellular functions and cell death: regulation and biological consequences. *Antioxid Redox Signal*. 2008;10:179–206.

8. Jope RS, Yuskaitis CJ, Beurel E. Glycogen synthase kinase-3 (GSK3): inflammation, diseases, and therapeutics. *Neurochem Res*. 2007;32(4-5):577–595.

9. Cohen P, Goedert M. GSK3 inhibitors: development and therapeutic potential. *Nat Rev Drug Discov*. 2004;3:479–487.

10. Jope RS, Johnson GV. The glamour and gloom of glycogen synthase kinase-3. *Trends Biochem Sci*. 2004;29:95–102.

11. Miura T, Miki T. GSK-3beta, a therapeutic target for cardiomyocyte protection. *Circ J*. 2009;73:1184–1192.

12. Gross ER, Hsu AK, Gross GJ. Opioid-induced cardioprotection occurs via glycogen synthase kinase beta inhibition during reperfusion in intact rat hearts. *Circ Res*. 2004;94:960–966.

13. Nishihara M, Miura T, Miki T, et al. Modulation of the mitochondrial permeability transition pore complex in GSK-3beta-mediated myocardial protection. *J Mol Cell Cardiol*. 2007;43:564–570.

14. Tong H, Imahashi K, Steenbergen C, Murphy E. Phosphorylation of glycogen synthase kinase-3beta during preconditioning through a phosphatidylinositol-3-kinase–dependent pathway is cardioprotective. *Circ Res*. 2002;90:377–379.

15. Hu B, Wu Y, Liu J, et al. GSK-3beta inhibitor induces expression of Nrf2/TrxR2 signaling pathway to protect against renal ischemia/reperfusion injury in diabetic rats. *Kidney Blood Press Res*. 2016;41:937–946.

16. Tanigawa S, Fujii M, Hou DX. Action of Nrf2 and Keap1 in ARE-mediated NQO1 expression by quercetin. *Free Radic Biol Med*. 2007;42:1690–1703.

17. Chen X, Liu Y, Zhu J, et al. GSK-3beta downregulates Nrf2 in cultured cortical neurons and in a rat model of cerebral ischemia-reperfusion. *Sci Rep*. 2016;6:20196.

18. Gao E, Lei YH, Shang X, et al. A novel and efficient model of coronary artery ligation and myocardial infarction in the mouse. *Circ Res*. 2010;107:1445–1453.

19. Jeong SH, Song IS, Kim HK, et al. An analogue of resveratrol HS-1793 exhibits anticancer activity against MCF-7 cells via inhibition of mitochondrial biogenesis gene expression. *Mol Cells*. 2012;34:357–365.

20. Ko TH, Marquez JC, Kim HK, et al. Resistance exercise improves cardiac function and mitochondrial efficiency in diabetic rat hearts. *Pflugers Arch*. 2018;470:263–275.

21. Davies SP, Reddy H, Caivano M, Cohen P. Specificity and mechanism of action of some commonly used protein kinase inhibitors. *Biochem J*. 2000;351(Pt 1):95–105.

22. Thu VT, Kim HK, Long le T, et al. NecroX-5 prevents hypoxia/reoxygenation injury by inhibiting the mitochondrial calcium uniporter. *Cardiovasc Res*. 2012;94:342–350.

23. Zeng M, Wei X, Wu ZY, et al. Simulated ischemia/reperfusion-induced p65-Beclin 1-dependent autophagic cell death in human

umbilical vein endothelial cells. *Sci Rep*. 2016;6:37448.

24. Morris GM, Green LG, Radic Z, et al. Automated docking with protein flexibility in the design of femtomolar "click chemistry" inhibitors of acetylcholinesterase. *J Chem Inf Model*. 2013;53:898–906.

25. Bertrand JA, Thieffine S, Vulpetti A, et al. Structural characterization of the GSK-3beta active site using selective and non-selective ATP-mimetic inhibitors. *J Mol Biol*. 2003;333:393–407.

26. Juhaszova M, Zorov DB, Yaniv Y, et al. Role of glycogen synthase kinase-3beta in cardioprotection. *Circ Res*. 2009;104:1240–1252.

27. Maejima Y, Galeotti J, Molkentin JD, Sadoshima J, Zhai P. Constitutively active MEK1 rescues cardiac dysfunction caused by overexpressed GSK-3alpha during aging and hemodynamic pressure overload. *Am J Physiol Heart Circ Physiol*. 2012;303:H979–H988.

28. Zhou J, Freeman TA, Ahmad F, et al. GSK-3alpha is a central regulator of age-related pathologies in mice. *J Clin Invest*. 2013;123:1821–1832.

29. Ahmad F, Singh AP, Tomar D, et al. Cardiomyocyte-GSK-3alpha promotes mPTP opening and heart failure in mice with chronic pressure overload. *J Mol Cell Cardiol*. 2019;130:65–75.

30. Nakamura M, Liu T, Husain S, et al. Glycogen synthase kinase-3alpha promotes fatty acid uptake and lipotoxic cardiomyopathy. *Cell Metab*. 2019;29:1119–1134. e12.

31. Ahmad F, Lal H, Zhou J, et al. Cardiomyocyte-specific deletion of Gsk3alpha mitigates post-myocardial infarction remodeling, contractile dysfunction, and heart failure. *J Am Coll Cardiol*. 2014;64:696–706.

32. Lal H, Zhou J, Ahmad F, et al. Glycogen synthase kinase-3alpha limits ischemic injury, cardiac rupture, post-myocardial infarction remodeling and death. *Circulation*. 2012;125:65–75.

33. Antos CL, McKinsey TA, Frey N, et al. Activated glycogen synthase-3 beta suppresses cardiac hypertrophy in vivo. *Proc Natl Acad Sci U S A*. 2002;99:907–912.

34. Hirotani S, Zhai P, Tomita H, et al. Inhibition of glycogen synthase kinase 3beta during heart failure is protective. *Circ Res*. 2007;101:1164–1174.

35. Murphy E, Steenbergen C. Inhibition of GSK-3 beta as a target for cardioprotection: the importance of timing, location, duration and degree of inhibition. *Exp Opin Ther Targets*. 2005;9:447–456.

36. Yang K, Chen Z, Gao J, et al. The key roles of GSK-3beta in regulating mitochondrial activity. *Cell Physiol Biochem*. 2017;44:1445–1459.

37. Zhu J, Rebecchi MJ, Glass PS, Brink PR, Liu L. Cardioprotection of the aged rat heart by GSK-3beta inhibitor is attenuated: age-related changes in mitochondrial permeability transition pore modulation. *Am J Physiol Heart Circ Physiol*. 2011;300:H922–H930.

38. Eldar-Finkelman H, Martinez A. GSK-3 inhibitors: preclinical and clinical focus on CNS. *Front Mol Neurosci*. 2011;4:32.

39. Martin SA, Souder DC, Miller KN, et al. GSK3beta regulates brain energy metabolism. *Cell Rep*. 2018;23:1922–1931.e4.

40. Walker MA, Tian R. Raising NAD in heart failure: time to translate? *Circulation*. 2018;137:2274–2277.

41. Canto C, Menzies KJ, Auwerx J. NAD^+ metabolism and the control of energy homeostasis: a balancing act between mitochondria and the nucleus. *Cell Metab*. 2015;22:31–53.

42. Mericskay M. Nicotinamide adenine dinucleotide homeostasis and signalling in heart disease: pathophysiological implications and therapeutic potential. *Arch Cardiovasc Dis*. 2016;109:207–215.

43. Diguet N, Trammell SAJ, Tannous C, et al. Nicotinamide riboside preserves cardiac function in a mouse model of dilated cardiomyopathy. *Circulation*. 2018;137:2256–2273.

44. Lee CF, Chavez JD, Garcia-Menendez L, et al. Normalization of NAD^+ redox balance as a therapy for heart failure. *Circulation*. 2016;134:883–894.

45. Dai X, Yan X, Zeng J, et al. Elevating CXCR7 improves angiogenic function of EPCs via Akt/GSK-3beta/Fyn-mediated Nrf2 activation in diabetic limb ischemia. *Circ Res*. 2017;120:e7–e23.

46. Khadka D, Kim HJ, Oh GS, et al. Augmentation of NAD^+ levels by enzymatic action of NAD(P)H quinone oxidoreductase 1 attenuates Adriamycin-induced cardiac dysfunction in mice. *J Mol Cell Cardiol*. 2018;124:45–57.

47. Lee TM, Lin SZ, Chang NC. Antiarrhythmic effect of lithium in rats after myocardial infarction by activation of Nrf2/HO-1 signaling. *Free Radic Biol Med*. 2014;77:71–81.

48. Lam AP, Gottardi CJ. β-Catenin signaling: a novel mediator of fibrosis and potential therapeutic target. *Curr Opin Rheumatol*. 2011;23:562–567.

49. Lehwald N, Tao GZ, Jang KY, et al. β-Catenin regulates hepatic mitochondrial function and energy balance in mice. *Gastroenterology*. 2012;143:754–764.

KEY WORDS GSK-3β inhibition, ischemia/reperfusion injury, marine pyridine α-nucleoside, mitochondria, NPS A

APPENDIX For a supplemental Methods section, figures, and references, please see the online version of this paper.